Leukocyte-mimetic liposomes possessing leukocyte membrane proteins pass through inflamed endothelial cell layer by regulating intercellular junctions

Tatsuya Fukuta,[1,*] Shintaro Yoshimi,[1] Tamotsu Tanaka,[1] Kentaro Kogure[1]

[1]*Graduate School of Biomedical Sciences, Tokushima University, Shomachi 1, Tokushima, 770-8505, Japan*

[*]Corresponding author: Tatsuya Fukuta

TEL: +81-88-633-7248

FAX: +81-88-633-9572

Email: fukuta.t@tokushima-u.ac.jp

Graduate School of Biomedical Sciences, Tokushima University, Shomachi 1, Tokushima, 770-8505, Japan

Abstract

Nanoparticles such as liposomes have been applied for the treatment of various diseases such as cancer and inflammatory diseases by utilizing the enhanced permeability and retention effect. However, their entry into inflammation sites is still limited since passive delivery of nanoparticles is often hampered by the presence of endothelial barriers. As leukocytes can pass through the inflamed endothelium via utilizing membrane protein functions, we hypothesized that incorporating leukocyte membrane proteins onto liposomal membranes may impart leukocyte-mimicking functions to liposomes, allowing for their adherence to and active passage through the inflamed endothelium. Herein, we developed leukocyte-mimetic liposomes (LM-Lipo) by leukocyte membrane protein transfer and evaluated their function *in vitro*. Transfer of membrane proteins from human leukemia cells onto liposomal membranes allowed for significant association of the liposomes with inflamed human endothelial cells, and subsequent passage through inflamed endothelial cell layer. The confocal images showed that LM-Lipo significantly induced vascular endothelial-cadherin displacement. These results indicate that LM-Lipo adhered to and regulated intercellular junctions of inflamed endothelial cell layer, resulting in passage through the layer, by mimicking the function of leukocytes. Furthermore, it is suggested that liposomes possessing leukocyte-like functions could be useful for drug delivery to inflammation sites by overcoming endothelial barriers.

Keywords

Liposome; Leukocyte; Intermembrane protein transfer; Inflamed endothelial cell layer; Vascular endothelial-cadherin; Inflammatory disease

Abbreviation: ATRA, all-trans retinoic acid; CD11a, lymphocyte function-associated antigen-1; CD11b, macrophage antigen-1; DCP, dicetylphosphate; $DiIC_{18}$, 1,1'-dioctadecyl-3,3,3',3'-tetramethylindocarbocyanine perchlorate; DMPC, dimyristoylphosphatidylcholine; DOPE, dioleoylphosphatidylethanolamine; EPC, egg

1 phosphatidylcholine; F-actin, filamentous actin; ICAM-1, intercellular adhesion molecule-1; HL-60,
2 human promyelocytic leukemia cell; HUVEC, human umbilical vein endothelial cell; TNF-α, tumor
3 necrosis factor-alpha; VE-cadherin, vascular endothelial-cadherin
4

1. Introduction

To develop new therapies for the treatment of a variety of diseases, delivery of drugs using nanoparticle drug delivery system (DDS), such as liposomes, has been broadly employed (Oku, 2017). For example, application of liposomes for cancer therapy is a well-known approach (Miao et al., 2015), and our previous studies demonstrated the applicability of liposomes for the treatment of cerebral ischemia/reperfusion injury, one of the inflammatory diseases (Fukuta et al., 2017; Ishii et al., 2012). The therapeutic approaches for cancer and certain inflammatory diseases are based on selective accumulation of liposomes in the diseased sites by passive extravasation through leaky blood vessels by the enhanced permeability and retention effect (Maeda et al., 2000). Also, to increase the accumulation amount and therapeutic efficacy of nanoparticles in the diseased sites, their modification with specific targeting ligands (e.g., antibodies and peptides) has been broadly reported (Byrne et al., 2008; Nishikawa et al., 2012; Zhao et al., 2016). However, nanoparticle entry into the sites of inflammation-related diseases is still limited since delivery of such nanoparticles to the diseased area is dependent on passive process and is often hampered by the presence of biological barriers including endothelial cells (Anselmo et al., 2015; Blanco et al., 2015). Thus, to achieve more secure drug delivery into the inflammation sites, functionalization of nanoparticles to allow for their active passage through the inflamed endothelial barriers is needed.

In recent years, focus has been on application of circulatory cells (e.g., red blood cells, leukocytes and platelets) as functional elements of drug carriers for the development of novel nanoparticles that utilize the properties of those cells, namely, biomimetic DDS (Anselmo and Mitragotri, 2014; Luk and Zhang, 2015). In particular, leukocytes are known to bind to inflamed endothelial cells via certain adhesion molecules, including intercellular adhesion molecule-1 (ICAM-1), and migrate to the site of inflammation, which leads to further pathological progression of inflammatory diseases via release of inflammatory mediators (Iadecola and Anrather, 2011; Vestweber, 2015). Indeed, it was reported that synthetic nanoparticles decorated with leukocyte membranes exhibit the ability to target inflamed tumor endothelium and to migrate into the diseased

area (Kang et al., 2017; Parodi et al., 2013). Based on these findings, we hypothesized that incorporation of leukocyte membrane proteins onto liposomal membranes may allow them to obtain leukocyte-mimicking functions, and facilitate the ability of the resultant liposomes to adhere to and actively pass through the inflamed endothelium around the diseased site, similar to leukocytes.

As mentioned above, imparting biomimetic properties to nanoparticles is expected to be an attractive strategy for targeted delivery to inflammation sites beyond the inflamed endothelial barrier. However, for bringing about biomimetic properties to nanoparticles, complicated processes, loss of protein activities, and difficulty in controlling physical properties (e.g., size and homogeneity) have been mentioned to be improved (Millan et al., 2004; Molinaro et al., 2016). It was previously reported that various membrane proteins can be spontaneously transferred to liposomal membranes without the need for solubilization and protein reconstitution steps using detergents, organic solvents, sonication, etc., a phenomenon known as intermembrane protein transfer (Huestis and Newton, 1986; Newton and Huestis, 1988). Since the transferred proteins retain their native activity and orientation in the lipid bilayer, intermembrane protein transfer was employed as a protein reconstitution method to provide functions to liposomes as well as other materials (Kogure et al., 1997b; Okumura et al., 1994). For example, a cancer vaccine was prepared by reconstitution of tumor antigens onto liposomes via intermembrane protein transfer, and was subsequently demonstrated to result in successful tumor regression in tumor model mice (Shibata et al., 1991). We previously also reported that transfer of an influenza virus fusion protein, namely hemagglutinin, to erythrocyte ghosts enabled the ghosts to fuse with cells, resulting in delivery of entrapped proteins into the cells (Kogure et al., 2000). Hence, this protein reconstitution method is considered a promising approach for easily imparting leukocyte-mimicking properties onto liposomes.

As one of the mechanisms of leukocyte passage through the inflamed endothelium following binding to adhesion molecules, interaction of membrane proteins, namely lymphocyte function-associated antigen-1 (LFA-1; CD11a) and macrophage antigen-1 (Mac-1; CD11b), with ICAM-1 was reported (Diamond et al., 1991; van Buul et al., 2007). When leukocytes adhere to

inflamed endothelium via binding of both CD11a and CD11b to ICAM-1, activation of the ICAM-1 signaling pathway is induced, leading to an increase in permeability of the endothelial cells and leukocyte infiltration into the inflammatory sites (Etienne-Manneville et al., 2000; Palomba et al., 2016). Therefore, transfer of leukocyte membrane proteins including both CD11a and CD11b onto liposomal membranes is considered to enable the liposomes to exhibit the ability to not only adhere to but also pass through the inflamed endothelium via interactions with ICAM-1. To this end, we used a human promyelocytic leukemia cell line, namely HL-60 cell, as a donor of leukocyte membrane proteins in this study, since HL-60 cells constitutively express CD11a. Additionally, CD11b expression can be induced by differentiation into neutrophil-like cells by the treatment with all-trans retinoic acid (ATRA) (Trayner et al., 1998). For evaluating the function of liposomes, we used tumor necrosis factor-α (TNF-α)-treated human umbilical vein endothelial cells (HUVECs) as a model of inflamed endothelium since treatment with TNF-α was reported to induce ICAM-1 expression in HUVECs (Ramana et al., 2004).

In the present study, we aimed to develop liposomes possessing leukocyte-mimicking functions, namely leukocyte-mimetic liposomes (LM-Lipo), via transfer of membrane proteins from HL-60 cells. Then, by using TNF-α-treated HUVECs as a model of inflamed endothelium, we investigated the ability of LM-Lipo to adhere to and actively pass through inflamed endothelial cell layer *in vitro*.

2. Material and Methods

2.1. Cell cultures

The human promyelocytic leukemia cell line, HL-60, and human umbilical vein endothelial cells (HUVECs) were purchased from DS Pharma Biomedical Co., Ltd (Osaka, Japan) and PromoCell GmbH (Heidelberg, Germany), respectively. HL-60 cells were cultured in RPMI-1640 medium (Nacalai tesque, Kyoto, Japan) supplemented with 10% fetal bovine serum, 100 U/mL penicillin (Gibco, MA, USA), and 100 μg/mL streptomycin (Gibco). HUVECs were cultured in endothelial growth medium (EGM-2, PromoCell GmbH) composed of endothelial basal medium (EBM-2, PromoCell GmbH), 30 μg/mL gentamicin sulfate (30 μg/mL)/amphotericin B (15 ng/mL) (GA-1000; Lonza, Tokyo, Japan) and endothelial cell growth medium-2 supplement pack (PromoCell GmbH). HUVECs used in the present study were between passage 3 and 6. The cells were cultured at 37ºC in a 5% CO_2 incubator.

2.2. Differentiation of HL-60 cells

HL-60 cells (1.0 x 10^6 cells/3 mL) seeded onto a 60-mm dish were incubated in RPMI-1640 medium containing 1 μM all-trans retinoic acid (ATRA; Wako Pure Chemical, Osaka, Japan) dissolved in dimethyl sulfoxide (DMSO; Wako Pure Chemical). The final concentration of DMSO in the media was 0.1%. For the non-differentiated group, cells were incubated with 0.1% DMSO. After incubation for 0, 24, 48, 72, 96, and 120 h, the cells were harvested and washed with phosphate-buffered saline (PBS). The cells were then incubated with Fc receptor blocking solution (Human TruStain FcX™; Biolegend, San Diego, CA, USA) at 4ºC for 10 min, followed by with Alexa Fluor 488-conjugated anti-human CD11b antibody (Biolegend) at 4ºC for 30 min. After washing the cells twice with PBS, the proportion of CD11b-positive cells, namely neutrophil-differentiated HL-60 cells, was measured by flow cytometry (Gallios; Beckman Coulter, CA, USA).

2.3. Western blotting

Anti-CD11a rabbit monoclonal antibody (ab52895; Abcam, Cambridge, UK), anti-CD11b rabbit monoclonal antibody (ab133357; Abcam), anti-β-actin mouse monoclonal antibody (sc-47778; Santa Cruz Biotechnology, CA, USA), horse-radish peroxidase (HRP)-conjugated anti-rabbit IgG polyclonal antibody (A24531; Thermo Fisher Scientific, Waltham, MA,USA), and HRP-conjugated anti-mouse IgG rabbit polyclonal antibody (ab97046; Abcam) were purchased from the sources indicated. To examine the expression of CD11a and CD11b in HL-60 cells, the media of the cells cultured in the presence of 1 μM ATRA or 0.1% DMSO for 96 h were removed following centrifugation at 1,000 *g* for 5 min at 4ºC. The cells were washed with PBS, centrifuged, and the supernatant was subsequently removed. This cycle was repeated three times. The cells were then lysed with lysis buffer comprised of 1% Triton-X100, 10 mM Tris (pH 7.5), 50 μg/mL aprotinin, 200 μM leupeptin, 2 mM phenylmethylsulfonyl fluoride, and 100 μM pepstatin A, followed by determination of protein concentration using a bicinchoninic acid (BCA) Protein Assay Reagent Kit (Pierce Biotechnology, Rockford, IL, USA). The resultant samples (10 μg protein) were subjected to 10% SDS-PAGE, and the proteins were electrophoretically transferred to a polyvinylidene difluoride (PVDF) membrane (Bio-Rad, Hercules, CA, USA). The PVDF membrane was incubated with 3% bovine serum albumin (BSA) dissolved in Tris-HCl-buffered saline containing 0.1% Tween20 (pH 7.4) for 1 h at 37ºC, followed by incubation with anti-CD11a at a dilution of 1:5000, anti-CD11b antibody (1:1000) or anti-β-actin antibody (1:20000) for 24 h at 4ºC, respectively. The PVDF membrane was then incubated with a secondary antibody at a dilution of 1: 2000 for rabbit IgG or 1:50000 for mouse IgG for 1 h at 37ºC. Each protein was detected using a LAS-4000 mini system (Fuji Film, Tokyo, Japan) after incubation with a chemiluminescent substrate reagent (ECL prime; GE Healthcare, Little Chalfont, UK).

2.4. Preparation of liposomes

Egg phosphatidylcholine (EPC) and dicetylphosphate (DCP) were purchased from

Sigma-Aldrich (Tokyo, Japan). Dioleoylphosphatidylethanolamine (DOPE) and dimyristoylphosphatidylcholine (DMPC) were purchased from NOF Corporation (Tokyo, Japan). Liposomes composed of EPC/DCP (7/3 molar ratio), EPC/DCP/DOPE (3.5/3/3.5 molar ratio), DMPC/DCP (7/3 molar ratio), and DMPC/DCP/DOPE (3.5/3/3.5 molar ratio) were prepared by the thin-film method. The above lipids dissolved in chloroform were added to test tubes and dried using nitrogen gas. To prepare fluorescence-labeled liposomes, 1, 1'-dioctadecyl-3,3,3',3'-tetramethylindocarbocyanine perchlorate ($DiIC_{18}$; Thermo Fisher Scientific, Waltham, MA, USA) dissolved in chloroform was added to the initial lipid solution at a concentration of 1 mol% of total lipid. The lipid film was hydrated with 0.3 M sucrose phosphate buffer (pH 7.4), and the liposomal suspensions were freeze-thawed for three cycles using dry-ice ethanol. The size of liposomes was then adjusted by extrusion through polycarbonate membrane filters with 100-nm pores (Nuclepore, Cambridge, MA, USA). The particle size and ζ-potential of the liposomes were measured with a Zetasizer Nano ZS (Malvern Instruments, Worcestershire, UK).

2.5. Intermembrane protein transfer

After culturing HL-60 cells in the presence of 1 μM ATRA or 0.1% DMSO for 96 h, the media were removed following centrifugation at 1,000 *g* for 5 min at 4ºC. The cells were washed with PBS and centrifuged, followed by removal of the supernatant. This cycle was repeated three times. Thereafter, the liposomal suspensions (1 mM as total lipids, 1 mL) were added and incubated with the cells (5 x 10^6 cells/1 mL of 1 mM liposomes) in a 35-mm dish for 90 min at 37ºC with shaking. As a control, 0.3 M sucrose phosphate buffer was also incubated with the cells. The incubated liposomes and 0.3 M sucrose phosphate buffer were harvested, centrifuged at 2,000 *g* for 1 min, and the supernatants were recovered and centrifuged to remove the cells. This cycle was repeated five times. The recovered samples were used in the following experiments.

2.6. Observation of protein transfer onto liposomes

To prepare the liposome samples for BCA assay and SDS-PAGE, 1 mL of the recovered liposomes (1 mM) following intermembrane transfer were ultracentrifuged at 112,500 *g* for 60 min at 4ºC (Optima L-90K; Beckman Coulter, Tokyo, Japan). The pellets of the liposomes were then resuspended in 100 μL of 0.3 M sucrose phosphate buffer to yield a liposome concentration of 10 mM. To prepare the control sample, the incubated and recovered 0.3 M sucrose phosphate buffer was also ultracentrifuged as described above. For determining protein concentration of the resultant liposomes, the liposomes were solubilized in 1% Triton-X100, and then protein concentration of each liposomal sample was measured by using a BCA Protein Assay Reagent Kit (Pierce Biotechnology, Rockford, IL, USA) according to the manufacturer's instructions. In the case of SDS-PAGE, the resultant samples (0.2 μmol as lipid concentration for the liposome samples or 10 μg protein for the cellular samples) were exposed to 10% SDS-PAGE. The proteins were then electrophoretically transferred to a PVDF membrane following SDS-PAGE. The PVDF membrane was then incubated with 3% BSA in Tris-buffered saline containing 0.1% Tween®20, each primary antibody, and secondary antibody, as described above. Finally, the proteins were incubated with ECL prime, and then detected with a LAS-4000 mini system. Quantification of signal intensities of each band in the images of Western blotting was performed by using an image-analysis system (ImageJ; National Institutes of Health, Bethesda, MD, USA). To calculate transfer efficiency of CD11a and CD11b onto liposomes, proportions of CD11a and CD11b in HL-60 cells were determined by silver staining (Silver Stain 2 Kit Wako, Wako Pure Chemical) following SDS-PAGE.

2.7. Evaluation of liposome association with HUVECs

HUVECs were seeded onto a 35-mm glass bottom dish at a density of 1 x 10^5 cells/dish and incubated overnight. The cells were then treated with TNF-α (10 ng/mL in EGM-2) for 16 h. $DiIC_{18}$ (DiI)-labeled liposomes composed of EPC/DCP/DOPE (3.5/3/3.5 molar ratio) or DMPC/DCP/DOPE (3.5/3/3.5 molar ratio) were incubated with non-differentiated or differentiated HL-60 cells as

described above (see Intermembrane protein transfer). Liposomes mixed in EBM-2 at a concentration at 0.5 mM (as total lipids) were added onto TNF-α-treated HUVECs for 3 h at 37ºC. After removing the liposomes and washing twice with PBS, the cells were fixed with 4% paraformaldehyde (PFA) for 1 h at 37ºC. The cells were then washed with PBS three times, and then incubated with PBS containing 0.1% Triton X100 for 15 min at 37ºC, followed by incubation with 1 μg/mL 4', 6-diamidino-2-phenylindole (DAPI; Thermo Fisher Scientific) in PBS for 15 min at 37ºC. After washing with PBS, the fluorescence was observed using a fluorescence microscope (Axio Vert.A1, Carl Zeiss, Jena, Germany).

To quantify the amount of the liposomes associated with HUVECs, the cells were seeded onto 24-well plate at a density of 5 x 10^4 cells/well, and treated with TNF-α as mentioned above. Following treatment with each liposomal sample for 3 h, the cells were washed with PBS and lysed with 1% n-octyl-β-D-glucoside (Dojindo, Kumamoto, Japan). The fluorescence intensity of DiI was determined using a Tecan Infinite M200 microplate reader (Salzburg, Männedorf, Switzerland). Thereafter, the total protein content was measured using a BCA Protein Assay Reagent Kit.

2.8. Transwell permeability assay

HUVECs were seeded onto a 6.5-mm Transwell plate with 8-μm pore polyester membrane inserts (Costar, Corning, Kennebunk, ME, USA) at a density of 2 x 10^5 cells/insert. The inserts were pre-incubated with 0.1% gelatin in PBS for 1 h at 37ºC, followed by EGM-2 overnight before seeding. At 48 h after seeding, the media on both the upper and bottom compartments were removed, and EGM-2 containing TNF-α (10 ng/mL) was then added to both compartments. At 16 h after incubation with TNF-α, the cells were treated with the liposomes (50 nmol as lipid dose/insert) incubated with non-differentiated or differentiated HL-60 cells, which liposomes were mixed in EBM-2 at a concentration of 0.5 mM. At 3 h after incubation, the media in the bottom comportment was collected and the DiI fluorescence was measured using a Tecan Infinite M200 microplate reader (excitation: 549 nm, emission: 592 nm).

2.9. Actin staining and immunostaining

HUVECs were seeded onto a 35-mm glass bottom dish coated with 0.1% gelatin and incubated overnight. The cells were treated with TNF-α and liposomes as described above (see Evaluation of liposome association with HUVECs). For filamentous actin (F-actin) staining, cells were treated with liposomes for 3 h at 37ºC, washed with PBS, and subsequently fixed in 4% PFA for 10 min at 37ºC following liposomal incubation. After washing twice with PBS, HUVECs were permeabilized with PBS containing 0.1% Triton-X100 for 5 min at 37ºC. The cells were then incubated in PBS containing 1% BSA for 20 min at 37ºC, followed by incubation with Alexa Fluor 488 phalloidin in PBS (1:40; Thermo Fisher Scientific) for 20 min at room temperature. After washing with PBS, the cells were stained with DAPI, and the fluorescence was observed by confocal laser scanning microscopy (LSM700, Carl Zeiss).

For immunostaining of vascular endothelial-cadherin (VE-cadherin), cells were washed with PBS, fixed with 4% PFA for 20 min at 37ºC, and permeabilized in PBS containing 1% BSA and 0.1% TritonX-100 for 20 min. The cells were then incubated with rabbit anti-VE-cadherin antibody (2.5 μg/mL; ab33168; Abcam) for 1 h at 37ºC, followed by washing with PBS containing 1% BSA and then incubation with Alexa Fluor 488-conjugated goat anti-rabbit IgG (1:200; ab150077; Abcam) for 1 h at 37ºC. After washing, the nuclei were stained with 1 μg/mL DAPI solution for 15 min at 37ºC. The fluorescence of the cells was monitored using a confocal laser scanning microscope. To evaluate level of VE-cadherin expression, the experiments were performed 5 times independently, and fluorescence intensities of VE-cadherin positive areas between cell borders were analyzed for total 40 or more images per each group of HUVECs using an image-analysis system ImageJ.

2.10. Statistical analysis

Statistical differences were evaluated by one-way analysis of variance (ANOVA) with the Tukey *post-hoc* test. Data were presented as mean ± S.D.

3. Results

3.1. Differentiation of HL-60 cells into neutrophil-like cells by ATRA

We firstly evaluated the differentiation of HL-60 cells into neutrophil-like cells by ATRA treatment for the preparation of donor cells to transfer the leukocyte membrane proteins CD11a and CD11b onto liposomal membranes. Flow cytometry results showed that cultivation of HL-60 cells in the presence of 1 μM ATRA significantly increased CD11b-positive cells in a time-dependent manner following initiation of ATRA treatment, whereas CD11b-positive cells did not increase in HL-60 cells cultured in the absence of ATRA (Figs. 1A and B). Since the percentage of CD11b-positive cells approached nearly 80% at 96 h after ATRA treatment and remained unchanged at 120 h (Fig. 1B), the differentiation of HL-60 cells into neutrophil-like cells was certainly achieved by the ATRA treatment for 96 h. Western blotting showed that HL-60 cells treated with ATRA for 96 h expressed both CD11a and CD11b, whereas those not treated with ATRA did not express CD11b (Fig. 1C). Based on these results, we decided to use those cells treated with ATRA for 96 h as neutrophil-differentiated cells, i.e., as donor cells of leukocyte membrane proteins, in subsequent experiments. On the other hand, the expression level of CD11a was significantly reduced to approximately 60% by the treatment with ATRA (Fig. 1D and Supplementary Fig. 1).

3.2. Intermembrane transfer of leukocyte membrane proteins from HL-60 cells onto liposomes

Using both differentiated and non-differentiated HL-60 cells, we examined the intermembrane protein transfer of membrane proteins onto liposomal membranes. Since the protein transfer was previously reported to be facilitated by increasing membrane fluidity of recipient liposomes (Waters et al., 1996), we prepared liposomes composed of EPC (containing unsaturated phospholipids) and liposomes composed of the saturated phospholipid DMPC to confirm the influence of membrane fluidity on protein transfer efficiency. Moreover, as previous studies reported that the efficiency of protein transfer to liposomes is increased by the presence of phase separation

via incorporation of the amphiphilic compound DCP into the liposomes (Kogure et al., 1997a; Kogure et al., 1999), we also prepared liposomes containing DCP. In addition, we incorporated the fusogenic phospholipid DOPE, because intermembrane protein transfer is induced by partial fusion between cellular membranes and liposomal membranes (Huestis and Newton, 1986; Newton and Huestis, 1988). Particle size, polydispersity index, and ζ-potential of liposomes used in the present study are shown in Table 1. The particle size and ζ-potential of each of the prepared liposomes was approximately 100-150 nm and -10 mV, respectively. To determine total protein concentration in the recovered liposome suspensions, BCA assay was performed for each liposome suspension incubated with differentiated or non-differentiated HL-60 cells. The results showed that the protein concentration tended to increase by incorporating DOPE in both EPC- and DMPC-based liposomes, and the concentrations were higher in the case of liposomal suspension been incubated with differentiated HL-60 cells (ATRA (+)) than that with non-differentiated cells (ATRA (-)) (Fig. 2). On the other hand, the particle sizes of the liposomes increased and the ζ-potentials became more negatively charged after incubation with HL-60 cells (Table 1).

Table 1. Physicochemical properties of liposomes before and after intermembrane protein transfer.

	Particle size (d. nm)		Polydispersity index		ζ-Potential (mV)	
	Before	After	Before	After	Before	After
EPC/DCP -Lipo	113.9±12.2	126.0±18.0	0.26±0.11	0.24±0.03	-9.7±1.0	-13.7±2.5
EPC/DCP/ DOPE-Lipo	109.6±12.2	150.7±14.4	0.21±0.09	0.35±0.08	-11.3±3.6	-16.0±1.8
DMPC/DCP -Lipo	145.0±28.0	185.0±61.1	0.37±0.11	0.49±0.13	-9.8±1.4	-13.3±1.4
DMPC/DCP/ DOPE-Lipo	119.2±12.2	140.3±17.1	0.24±0.12	0.35±0.08	-10.9±2.7	-15.1±2.4

Next, transfer of CD11a and CD11b onto liposomes was evaluated by Western blotting. The results of Western blotting showed that the presence of CD11a was observed in liposomal samples incubated with HL-60 cells (Fig. 3A). Importantly, CD11b was only observed in those liposomes incubated with ATRA-treated neutrophil-differentiated HL-60 cells (Fig. 3B). Considering the differences in liposome composition, in the groups of liposomes containing DOPE, both CD11a and CD11b were more clearly detected compared with the groups of liposomes containing only DCP (EPC/DCP-Lipo and DMPC/DCP-Lipo). However, neither CD11a nor CD11b was observed upon incubation of the cells with 0.3 M sucrose phosphate buffer. Quantitative data of Western blotting indicated that transfer amount of CD11a was significantly higher in the group of EPC/DCP/DOPE-Lipo compared with EPC/DCP-Lipo and DMPC/DCP-Lipo, and also higher than that of DMPC/DCP/DOPE-Lipo (Figs. 3C and D). In the case of CD11b, its transfer amount tended to be higher in the groups of liposomes containing DOPE (Fig. 3E). Since proportions of CD11a and CD11b in HL-60 cells were indicated to be approximately 1 % from silver staining following SDS-PAGE (data not shown), transfer efficiency of HL-60 cell membrane proteins, and that of CD11a and CD11b onto liposomes was estimated as shown in Supplementary Table 1. The data also indicated that incorporation of DOPE into liposomes could increase transfer efficiency of both CD11a and CD11b. Based on these results, it was indicated that transfer of leukocyte membrane proteins CD11a and CD11b onto liposomes was achieved by intermembrane protein transfer. The resultant liposomes possessing leukocyte membrane proteins were designated as “leukocyte-mimetic liposomes (LM-Lipo)”. EPC/DCP/DOPE-Lipo (EPC/DO-Lipo) and DMPC/DCP/DOPE-Lipo (DMPC/DO-Lipo) were used in subsequent experiments.

3.3. Association of leukocyte-mimetic liposomes (LM-Lipo) with TNF-α-treated HUVECs

Next, association of LM-Lipo with inflamed endothelial cells was investigated using TNF-α-treated HUVECs as an *in vitro* model, since it has been reported that treatment with TNF-α can induce ICAM-1 expression in HUVECs (Ramana et al., 2004). We confirmed that expression of

ICAM-1 was time-dependently and significantly increased at 16 h after TNF-α treatment, at which point ICAM-1 expression became the highest under the experimental conditions (Supplementary Fig. 2). By using fluorescence (DiI)-labeled liposomes, we evaluated the association of LM-Lipo with TNF-α-treated HUVECs using a fluorescence microscope. The results showed that the DiI fluorescence of HUVECs treated with leukocyte-mimetic EPC/DO-Lipo (LM-EPC/DO-Lipo) or DMPC/DO-Lipo (LM-DMPC/DO-Lipo) was stronger than plain liposomes regardless of whether HL-60 cells had been differentiated (ATRA (+)) or not (ATRA (-)) (Figs. 4A, B, D, and E). Importantly, higher fluorescence intensities were observed for TNF-α-treated HUVECs in both the LM-EPC/DO-Lipo and LM-DMPC/DO-Lipo groups compared with untreated HUVECs. The confocal images also showed that DiI fluorescences in TNF-α-treated HUVECs incubated with LM-EPC/DO-Lipo (ATRA (-)) and ATRA (+)) or LM-DMPC/DO-Lipo (ATRA (+)) were higher than plain liposomes (Supplementary Fig. 3). Also, some areas with higher fluorescence than other areas were observed, which were considered to be resulted from the liposomes localized in endosomes. The DiI fluorescence was also determined by lysing the cells, and the results indicated that the fluorescence intensity of the cells treated with LM-Lipo was significantly higher than that with plain liposomes in TNF-α-treated HUVECs (Figs. 4C and F). Moreover, LM-EPC/DO-Lipo incubated with non-differentiated (LM-EPC/DO-Lipo ATRA (-)) or differentiated HL-60 cells (LM-EPC/DO-Lipo ATRA (+)) and LM-DMPC/DO-Lipo (ATRA (+)) had significantly higher affinity to TNF-α-treated HUVECs compared with untreated ones, suggesting that those negatively charged liposomes attained leukocyte-mimetic properties to facilitate their adherence to inflamed endothelial cells. Because LM-DMPC/DO-Lipo showed lower affinity to TNF-α-treated HUVECs than LM-EPC/DO-Lipo, LM-EPC/DO-Lipo were used in subsequent experiments.

3.4. Passage of leukocyte-mimetic liposomes through TNF-α-treated HUVECs

Next, the ability of LM-Lipo to pass through inflamed endothelial cell layer was evaluated using TNF-α-treated HUVECs seeded onto Transwell inserts. DiI-labeled LM-Lipo were added onto

the upper compartments of the TNF-α-treated HUVECs cultured on the inserts, and the DiI fluorescence of the media in the bottom compartments was measured 3 h after liposomal treatment. The results showed that there was almost no difference between the groups of cells treated with EPC/DO-Lipo or LM-EPC/DO-Lipo (ATRA (-)), whereas the fluorescence intensity in the bottom compartment was higher in the LM-EPC/DO-Lipo (ATRA (+))-treated group compared with that in the EPC/DO-Lipo-treated group (Fig. 5). These results suggest that LM-EPC/DO-Lipo (ATRA (+)) not only adhered to but also passed through inflamed endothelial cell layer.

3.5. Influence of leukocyte-mimetic liposomes on cytoskeleton and intercellular adhesion junctions of inflamed endothelial cells

To analyze the mechanism of passage of LM-EPC/DO-Lipo (ATRA (+)) through the TNF-α-treated HUVEC layer, we investigated the influence of liposomal treatment on the cytoskeleton and intercellular adhesion junctions of inflamed endothelial cells. Confocal images of F-actin staining showed that the treatment with LM-EPC/DO-Lipo, especially LM-EPC/DO-Lipo (ATRA (+)), induced intracellular morphological changes of F-actin in TNF-α-treated HUVECs compared with non-treated HUVECs (Figs. 6A-D). As shown in Figure 6D, in the HUVECs treated with LM-EPC/DO-Lipo (ATRA (+)), the state of F-actin was changed and became sharp-shaped structures, and intracellular fluorescence derived from F-actin (Alexa Fluor 488 phalloidin) decreased compared with control (TNF-α (-)) and EPC/DO-Lipo groups.

We then evaluated the effect of treatment with LM-Lipo on the state of the intercellular adhesion protein, VE-cadherin, in TNF-α-treated HUVECs. Confocal images showed that expression of VE-cadherin and cell borders were clearly observed in normal HUVECs (Fig. 7A). Although the apparent formation of intercellular junctions was observed in TNF-α-treated cells treated with plain EPC/DO-Lipo (Fig. 7B), the fluorescence signals derived from VE-cadherin expression was decreased in the LM-EPC/DO-Lipo (ATRA (-))-treated cells, and the intercellular adhesions were also slightly compromised (Fig. 7C). Importantly, treatment with LM-EPC/DO-Lipo (ATRA (+))

markedly perturbed VE-cadherin expression and the formation of intercellular junctions compared to the other groups (Fig. 7D). The quantification data also indicated that the level of VE-cadherin expression in TNF-α-treated HUVECs incubated with LM-EPC/DO-Lipo (ATRA (+)) was significantly lower than the HUVECs incubated with plain EPC/DO-Lipo, and tended to be decreased compared with the cells treated with LM-EPC/DO-Lipo (ATRA (-)) (Fig. 7E). On the other hand, the expression of VE-cadherin was almost not changed by the treatment with EPC/DO-Lipo in the absence of TNF-α (Supplementary Figs. 5A and B). We also confirmed that HL-60 cells could induce morphological change of F-actin in TNF-α-treated HUVECs and the state of F-actin became sharp-shaped structures (Supplementary Fig. 4). In addition, the expression of VE-cadherin decreased in the TNF-α-treated HUVECs incubated with HL-60 cells, especially with ATRA-treated (differentiated) HL-60 cells, in comparison to HUVECs treated with TNF-α alone (Supplementary Figs. 5C and D), as reported previously in leukocytes (Isac et al., 2011; Vestweber, 2012). These results suggest that the LM-EPC/DO-Lipo (ATRA (+)) regulates intercellular junctions of the TNF-α-treated HUVECs by exerting functions of both CD11a and CD11b derived from neutrophil-differentiated HL-60 cells.

4. Discussion

Since accumulation of nanoparticles into the sites of tumor and inflammation is dependent on passive process, design of nanoparticles which can actively overcome the inflamed endothelium and accumulate in the diseased area is required (Anselmo et al., 2015; Blanco et al., 2015). Leukocytes are known to adhere to and pass through the inflamed endothelium via the interaction of their membrane proteins and adhesion molecules expressed on the endothelial cells (Etienne-Manneville et al., 2000; Vestweber, 2015). Thus, we hypothesized that incorporation of leukocyte membrane proteins onto liposomes could enable the liposomes to mimic the function of leukocytes, and thus allow for their active passage through the inflamed endothelium. Herein, we employed intermembrane protein transfer as a protein reconstitution method to impart nanoparticles with biomimetic properties, since this method is reported to be able to transfer cellular membrane proteins onto liposomal membranes with native orientation and activities (Huestis and Newton, 1986; Newton and Huestis, 1988). In the present study, we used liposomes containing the amphiphilic compound DCP because it was previously revealed that incorporation of DCP into liposomes induces phase separation of the liposomal membrane, resulting in increase in the efficiency of membrane protein transfer (Kogure et al., 1997a; Kogure et al., 1999). Similar to the previous studies, results shown in Fig. 3 confirmed the transfer of the membrane proteins of neutrophil-differentiated HL-60 cells, CD11a and CD11b, onto liposomes containing DCP. Additionally, the results of Western blotting showed that the transfer was more clearly observed in the group of liposomes composed of EPC than liposomes composed of DMPC (Figs. 3A and B). These results are consistent with a previous report, which showed that protein transfer is facilitated by increasing the membrane fluidity of the liposomes (Waters et al., 1996). In particular, when the fusogenic unsaturated phospholipid DOPE was incorporated into liposomes, higher transfer efficiency was observed both in EPC- and DMPC-based liposomes (Figs. 2 and 3). In fact, the amounts of total proteins, CD11a, and CD11b in the liposome suspensions collected after incubation with the cells tended to be higher both in EPC- and DMPC-based liposomes containing DOPE (Supplementary Table. 1). These results suggest that

incorporation of DOPE into liposomes could increase the efficiency of intermembrane protein transfer.

As shown in Fig. 1D and supplementary Fig. 1, differentiation of HL-60 cells by ATRA treatment significantly reduced CD11a expression levels to approximately 60% of non-differentiated HL-60 cells, although CD11b expression was induced by ATRA treatment (Figs. 1A-C). On the other hand, the amount of CD11a transferred onto liposomes from ATRA-treated differentiated HL-60 cells were larger than or almost same as that from non-differentiated cells (Supplementary Table 1), despite the CD11a expression level in differentiated HL-60 cells been lower than that in non-differentiated cells. From these results, it is considered that transfer efficiency of cellular membrane proteins via intermembrane protein transfer would be changed by the state of donor cells.

Leukocytes are known to adhere to inflamed endothelium and infiltrate into the site of inflammation by utilizing the functions of their carbohydrate chains and membrane proteins. In particular, the membrane proteins CD11a and CD11b, which were shown to be expressed in ATRA-induced neutrophil-differentiated HL-60 in our present study (Fig. 1) as well as in previous reports (Gee et al., 2012), have been reported to interact with ICAM-1 (Diamond et al., 1991; van Buul et al., 2007). Thus, to evaluate the leukocyte-mimicking ability of LM-Lipo, we first examined the association of the liposomes with inflamed endothelial cells using TNF-α-treated HUVECs, which express ICAM-1 as shown in Supplementary Fig. 2. The results showed that LM-Lipo significantly associated with the TNF-α-treated HUVECs compared with plain liposomes (Fig. 4). In addition, the liposomes showed significantly higher affinity to TNF-α-treated HUVECs than to untreated HUVECs (Fig. 4). Since CD11a has been reported to be involved in leukocyte adhesion to inflamed endothelium, it is considered that liposomes incubated with non-differentiated HL-60 cells could also significantly associate with TNF-α-treated HUVECs. These results suggest that liposomes possessing leukocyte membrane proteins could attain leukocyte-mimetic functions and selectively adhere to inflamed endothelial cells via ICAM-1. Moreover, it was confirmed that the transferred membrane proteins CD11a and CD11b could retained their functionalities and native orientations on

the liposomal membranes.

In the present study, LM-EPC/DO-Lipo (ATRA (+)) demonstrated an ability to pass through TNF-α-treated HUVEC layer cultured onto a Transwell plate compared with plain EPC/DO-Lipo (Fig. 5). As one of the mechanisms of leukocyte extravasation across inflamed endothelium via binding to adhesion molecules, it has been demonstrated that interaction of CD11a and CD11b on leukocytes with ICAM-1 on endothelial cells induces activation of the ICAM-1 signaling pathway (Palomba et al., 2016). This activation leads to a subsequent increase in intracellular calcium concentration, protein kinase C-α activation, and phosphorylation of VE-cadherin, which results in displacement of VE-cadherin and formation of gaps between the inflamed endothelial cells (Sandoval et al., 2001; Turowski et al., 2008). It has also been reported that when leukocytes pass through inflamed endothelium via the paracellular route, actin depolymerization is induced in addition to displacement of intercellular junction proteins (Mamdouh et al., 2009). In fact, the displacement of VE-cadherin and decrease in its expression level, and change of actin cytoskeleton were seen in TNF-α-treated HUVECs incubated with LM-Lipo possessing both CD11a and CD11b (Figs. 6 and 7). Based on these results, it is suggested that interaction of both CD11a and CD11b on LM-Lipo with ICAM-1 resulted in activation of the ICAM-1 signaling pathway by exerting their functions. This signal activation subsequently induced displacement of VE-cadherin and increased the permeability between the cells, resulting in passage of LM-Lipo through the inflamed HUVEC layer.

Liposomes could attain leukocyte-mimicking abilities by reconstitution of leukocyte membrane proteins, especially CD11a and CD11b, via intermembrane protein transfer. Since the protein reconstitution method nonspecifically transfers membrane proteins onto liposomes, other proteins might interact with other endothelial adhesion molecules involved in leukocyte extravasation (Vestweber, 2015). However, it is possible that modification of the liposome surface with both CD11a and CD11b, or peptides containing ICAM-1 recognition domains that subsequently activate the ICAM-1 signaling pathway, similar to the membrane proteins, could allow for adhesion

to inflamed endothelial cells and perturbation of intercellular junctions, leading to passage of the nanoparticles through endothelial cell layer into inflammation sites. Design of such nanoparticles should be both useful and interesting for future studies.

LM-EPC/DO-Lipo (ATRA (+)) developed in this study exhibited leukocyte-mimicking properties by regulating cellular junctions of inflamed endothelial cells and passing through the endothelial cell layer. Hence, LM-Lipo has the potential to be useful in applications for the treatment of inflammatory diseases, similar to leukocytes invading the inflammation sites. In previous reports, leukocyte-mimetic nanoparticles were prepared via complicated steps, i.e., collection and purification of cellular membrane fractions from cell lysates by density gradient centrifugation, followed by their modification onto nanoparticles by chemical conjugation or physical processes such as sonication and extrusion (Kang et al., 2017; Parodi et al., 2013). On the other hand, the intermembrane protein transfer employed in the present study has the advantage that cellular membrane proteins can be easily transferred with their native activity and orientation by only incubating the liposomes with the cells (Huestis and Newton, 1986; Shibata et al., 1991). Also, our present study demonstrated that it is possible to construct biomimetic DDS even by such a more simple method than conventional methods reported previously. *In vivo* applications using leukocytes derived from animal blood should be considered a necessary next step in demonstrating further utility of LM-Lipo. Since inflammation has been reported to be involved in the pathological progression of a number of diseases (Chu et al., 2015; Eltzschig and Eckle, 2011; Maeda et al., 2013), application of LM-Lipo could become a hopeful approach for developing treatments for such diseases.

5. Conclusions

In summary, development of LM-Lipo could be achieved by intermembrane transfer of leukocyte membrane proteins onto liposomal membranes. LM-Lipo was able to associate with TNF-α-treated ICAM-1-expressing HUVECs and pass through the cell layer by exerting the functions of leukocyte membrane proteins. Moreover, the mechanism of passage is considered to be due to the displacement of VE-cadherin accompanying change of actin cytoskeleton by interaction of both CD11a and CD11b with ICAM-1. Hence, the present findings suggest that imparting leukocyte-mimetic properties onto liposomes represents a promising approach to overcome endothelial barriers by regulating intercellular junctions, and that LM-Lipo could be a useful DDS for developing a new therapy for the treatment of inflammatory diseases.

Acknowledgement

This research was supported by a Grant-in-Aid for Scientific Research from the Japan Society for the Promotion of Science (JSPS, No. 17H06906). The authors are also thankful for support from the Research Program for the Development of Intelligent Tokushima Artificial Exosome (iTEX) from Tokushima University.

Author contributions

TF and KK designed the research. TF and SY performed the experiments. TF and TT analyzed the data. TF and KK wrote the paper.

References

Anselmo, A.C., Gilbert, J.B., Kumar, S., Gupta, V., Cohen, R.E., Rubner, M.F., Mitragotri, S., 2015. Monocyte-mediated delivery of polymeric backpacks to inflamed tissues: a generalized strategy to deliver drugs to treat inflammation. J Control Release 199, 29-36.

Anselmo, A.C., Mitragotri, S., 2014. Cell-mediated delivery of nanoparticles: taking advantage of circulatory cells to target nanoparticles. J Control Release 190, 531-541.

Blanco, E., Shen, H., Ferrari, M., 2015. Principles of nanoparticle design for overcoming biological barriers to drug delivery. Nat Biotechnol 33, 941-951.

Byrne, J.D., Betancourt, T., Brannon-Peppas, L., 2008. Active targeting schemes for nanoparticle systems in cancer therapeutics. Adv Drug Deliv Rev 60, 1615-1626.

Chu, D., Gao, J., Wang, Z., 2015. Neutrophil-mediated delivery of therapeutic nanoparticles across blood vessel barrier for treatment of inflammation and infection. ACS nano 9, 11800-11811.

Diamond, M.S., Staunton, D.E., Marlin, S.D., Springer, T.A., 1991. Binding of the integrin Mac-1 (CD11b/CD18) to the third immunoglobulin-like domain of ICAM-1 (CD54) and its regulation by glycosylation. Cell 65, 961-971.

Eltzschig, H.K., Eckle, T., 2011. Ischemia and reperfusion--from mechanism to translation. Nat Med 17, 1391-1401.

Etienne-Manneville, S., Manneville, J.B., Adamson, P., Wilbourn, B., Greenwood, J., Couraud, P.O., 2000. ICAM-1-Coupled Cytoskeletal Rearrangements and Transendothelial Lymphocyte Migration Involve Intracellular Calcium Signaling in Brain Endothelial Cell Lines. J Immunol 165, 3375-3383.

Fukuta, T., Asai, T., Yanagida, Y., Namba, M., Koide, H., Shimizu, K., Oku, N., 2017. Combination therapy with liposomal neuroprotectants and tissue plasminogen activator for treatment of ischemic stroke. FASEB J 31, 1879-1890.

Gee, D.J., Wright, L.K., Zimmermann, J., Cole, K., Soule, K., Ubowski, M., 2012. Dimethylsulfoxide exposure modulates HL-60 cell rolling interactions. Biosci Rep 32, 375-382.

Huestis, W.H., Newton, A., 1986. Intermembrane protein transfer. Band 3, the erythrocyte anion

transporter, transfers in native orientation from human red blood cells into the bilayer of phospholipid vesicles. J Biol Chem 261, 16274-16278.

Iadecola, C., Anrather, J., 2011. The immunology of stroke: from mechanisms to translation. Nat Med 17, 796-808.

Isac, L., Thoelking, G., Schwab, A., Oberleithner, H., Riethmuller, C., 2011. Endothelial f-actin depolymerization enables leukocyte transmigration. Anal Bioanal Chem 399, 2351-2358.

Ishii, T., Asai, T., Oyama, D., Fukuta, T., Yasuda, N., Shimizu, K., Minamino, T., Oku, N., 2012. Amelioration of cerebral ischemia-reperfusion injury based on liposomal drug delivery system with asialo-erythropoietin. J Control Release 160, 81-87.

Kang, T., Zhu, Q., Wei, D., Feng, J., Yao, J., Jiang, T., Song, Q., Wei, X., Chen, H., Gao, X., Chen, J., 2017. Nanoparticles Coated with Neutrophil Membranes Can Effectively Treat Cancer Metastasis. ACS Nano 11, 1397-1411.

Kogure, K., Itoh, T., Okuda, O., Hayashi, K., Ueno, M., 2000. The delivery of protein into living cells by use of membrane fusible erythrocyte ghosts. Int J Pharm 210, 117-120.

Kogure, K., Nakamura, C., Okuda, O., Hayashi, K., Ueno, M., 1997a. Effect of dicetylphosphate or stearic acid on spontaneous transfer of protein from influenza virus-infected cells to dimyristoylphosphatidylcholine liposomes. Biochim Biophys Acta Biomembr 1329, 174-182.

Kogure, K., Okuda, O., Itoh, T., Hayashi, K., Ueno, M., 1997b. Development of a membrane fusible drug carrier from erythrocytes by the spontaneous transfer of viral fusion protein from influenza virus-infected cells. Biol Pharm Bull 20, 581-583.

Kogure, K., Okuda, O., Nakamura, C., Hayashi, K., Ueno, M., 1999. Effects of Incorporation of Various Amphiphiles into Recipient Liposome Membraneson Inter-Membrane Protein Transfer. Chem Pharm Bull 47, 1117-1120.

Luk, B.T., Zhang, L., 2015. Cell membrane-camouflaged nanoparticles for drug delivery. J Control Release 220, 600-607.

Maeda, H., Nakamura, H., Fang, J., 2013. The EPR effect for macromolecular drug delivery to solid

tumors: Improvement of tumor uptake, lowering of systemic toxicity, and distinct tumor imaging in vivo. Adv Drug Deliv Rev 65, 71-79.

Maeda, H., Wu, J., Sawa, T., Matsumura, Y., Hori, K., 2000. Tumor vascular permeability and the EPR effect in macromolecular therapeutics: a review. J Control Release 65, 271-284.

Mamdouh, Z., Mikhailov, A., Muller, W.A., 2009. Transcellular migration of leukocytes is mediated by the endothelial lateral border recycling compartment. J Exp Med 206, 2795-2808.

Miao, L., Lin, C.M., Huang, L., 2015. Stromal barriers and strategies for the delivery of nanomedicine to desmoplastic tumors. J Control Release 219, 192-204.

Millan, C.G., Marinero, M.L., Castaneda, A.Z., Lanao, J.M., 2004. Drug, enzyme and peptide delivery using erythrocytes as carriers. J Control Release 95, 27-49.

Molinaro, R., Corbo, C., Martinez, J.O., Taraballi, F., Evangelopoulos, M., Minardi, S., Yazdi, I.K., Zhao, P., De Rosa, E., Sherman, M.B., De Vita, A., Toledano Furman, N.E., Wang, X., Parodi, A., Tasciotti, E., 2016. Biomimetic proteolipid vesicles for targeting inflamed tissues. Nat Mater 15, 1037-1046.

Newton, A.C., Huestis, W.H., 1988. Lymphoma-vesicle interactions: vesicle adsorption, membrane fragmentation, and intermembrane protein transfer. Biochemistry 27, 4645-4655.

Nishikawa, K., Asai, T., Shigematsu, H., Shimizu, K., Kato, H., Asano, Y., Takashima, S., Mekada, E., Oku, N., Minamino, T., 2012. Development of anti-HB-EGF immunoliposomes for the treatment of breast cancer. J Control Release 160, 274-280.

Oku, N., 2017. Innovations in liposomal DDS technology and its application for the treatment of various diseases. Biol Pharm Bull 40, 119-127.

Okumura, Y., Ishitobi, M., Sobel, M., Akiyoshi, K., Sunamoto, J., 1994. Transfer of membrane proteins from human platelets to liposomal fraction by interaction with liposomes containing an artificial boundary lipid. Biochim Biophys Acta Biomembr 1194, 335-340.

Palomba, R., Parodi, A., Evangelopoulos, M., Acciardo, S., Corbo, C., de Rosa, E., Yazdi, I.K., Scaria, S., Molinaro, R., Furman, N.E., You, J., Ferrari, M., Salvatore, F., Tasciotti, E., 2016.

Biomimetic carriers mimicking leukocyte plasma membrane to increase tumor vasculature permeability. Sci Rep 6, 34422.

Parodi, A., Quattrocchi, N., van de Ven, A.L., Chiappini, C., Evangelopoulos, M., Martinez, J.O., Brown, B.S., Khaled, S.Z., Yazdi, I.K., Enzo, M.V., Isenhart, L., Ferrari, M., Tasciotti, E., 2013. Synthetic nanoparticles functionalized with biomimetic leukocyte membranes possess cell-like functions. Nat Nanotechnol 8, 61-68.

Ramana, K.V., Bhatnagar, A., Srivastava, S.K., 2004. Inhibition of aldose reductase attenuates TNF-alpha-induced expression of adhesion molecules in endothelial cells. FASEB J 18, 1209-1218.

Sandoval, R., Malik, A.B., Minshall, R.D., Kouklis, P., Ellis, C.A., Tiruppathi, C., 2001. Ca2+ signalling and PKCα activate increased endothelial permeability by disassembly of VE—cadherin junctions. J Physiol 533, 433-445.

Shibata, R., Noguchi, T., Sato, T., Akiyoshi, K., Sunamoto, J., Shiku, H., Nakayama, E., 1991. Induction of in vitro and in vivo anti‐tumor responses by sensitization of mice with liposomes containing a crude butanol extract of leukemia cells and transferred inter‐membranously with cell‐surface proteins. Int J Cancer 48, 434-442.

Trayner, I.D., Bustorff, T., Etches, A.E., Mufti, G.J., Foss, Y., Farzaneh, F., 1998. Changes in antigen expression on differentiating HL60 cells treated with dimethylsulphoxide, all-trans retinoic acid, α1, 25-dihydroxyvitamin D3 or 12-O-tetradecanoyl phorbol-13-acetate. Leukemia research 22, 537-547.

Turowski, P., Martinelli, R., Crawford, R., Wateridge, D., Papageorgiou, A.P., Lampugnani, M.G., Gamp, A.C., Vestweber, D., Adamson, P., Dejana, E., Greenwood, J., 2008. Phosphorylation of vascular endothelial cadherin controls lymphocyte emigration. J Cell Sci 121, 29-37.

van Buul, J.D., Kanters, E., Hordijk, P.L., 2007. Endothelial signaling by Ig-like cell adhesion molecules. Arterioscler Thromb Vasc Biol 27, 1870-1876.

Vestweber, D., 2012. Relevance of endothelial junctions in leukocyte extravasation and vascular permeability. Ann N Y Acad Sci 1257, 184-192.

Vestweber, D., 2015. How leukocytes cross the vascular endothelium. Nat Rev Immunol 15,

692-704.

Waters, S.I., Sen, R., Brunauer, L.S., Huestis, W.H., 1996. Physical Determinants of Intermembrane Protein Transfer. Biochemistry 35, 4002-4008.

Zhao, Y., Jiang, Y., Lv, W., Wang, Z., Lv, L., Wang, B., Liu, X., Liu, Y., Hu, Q., Sun, W., Xu, Q., Xin, H., Gu, Z., 2016. Dual targeted nanocarrier for brain ischemic stroke treatment. J Control Release 233, 64-71.

Figure legends

Figure 1. Differentiation of HL-60 cells into neutrophil-like cells by treatment with ATRA.

(A) HL-60 cells (1.0 x 10^6 cells/60-mm dish) were treated with 1 μM ATRA for 0, 24, 48, 72, 96, or 120 h to induce differentiation into neutrophil-like cells. In the non-differentiated group, the cells were cultured in the presence of 0.1% DMSO. Following incubation, the cells were collected and stained with Alexa Fluor 488-conjugated anti-CD11b antibody. Thereafter, flow cytometric analysis was performed to measure the CD11b-positive cells. The white and gray histograms indicate cells treated without and with ATRA, respectively. (B) The percentage of CD11b-positive (neutrophil-differentiated) cells was determined from the histogram data. The data show the mean ± S.D. (n=3). (C, D) Expression of CD11b (Mac-1; C) and CD11a (LFA-1; D) in ATRA-treated and non-ATRA-treated groups was determined by Western blotting after incubation for 96 h. The experiments of Western blotting were performed 3 times independently.

Figure 2. Determination of protein concentration of the recovered liposome suspensions after incubation with HL-60 cells.

Liposomes consisted of each lipid composition were incubated for 90 min with HL-60 cells cultivated in the presence or absence of ATRA for 96 h. Protein concentrations of the recovered

liposomes incubated with non-differentiated HL-60 cells (ATRA (-)) or differentiated HL-60 cells (ATRA (+)) were determined by BCA assay. The data show the mean ± S.D. (n=4). The experiments were conducted 4 times independently.

Figure 3. Transfer of leukocyte membrane proteins onto liposomes via intermembrane protein transfer with HL-60 cells.

(A, B) Liposomes comprised of each lipid composition or 0.3 M sucrose phosphate buffer were incubated with non-differentiated (ATRA (-)) or neutrophil-differentiated (ATRA (+)) HL-60 cells for 90 min. Each lane indicates a specific liposome (0.2 μmol as total lipid) or cell extract of differentiated HL-60 cells (10 μg protein) that was subjected to SDS-PAGE. Western blot analysis was then performed to confirm the transfer of CD11a (A) and CD11b (B) onto the liposomes. Per the product datasheet, the detected molecular weights of CD11a and CD11b are approximately 180 kDa and 170 kDa, respectively. The bands in the leftmost lane correspond to the Western Protein Standard (MagicMark^{TM} XP; Thermo Fisher Scientific). (C-E) The signal intensities of the bands of CD11a (C; ATRA (-), D; ATRA (+)) and CD11b (E) transferred onto liposomes were calculated by using an image-analysis system Image J. The relative signal intensities of each band to that of differentiated HL-60 cells are presented. The data show the mean ± S.D. (C and D; n=3, E; n=4). Statistical differences were analyzed by ANOVA with Tukey *post-hoc* test. Significant differences; * $P<0.05$, ** $P<0.01$. The experiments were performed 3 for A, C, and D and 4 times for B and E.

Figure 4. Association of leukocyte-mimetic liposomes with TNF-α-treated inflamed HUVECs.

(A, B, D, E) HUVECs (1 x 10^5 cells/35-mm dish) were treated with TNF-α (10 ng/mL in EGM) for 16 h at 37ºC to induce expression of ICAM-1, as shown in Supplementary Fig. 2. DiI-labeled EPC/DO-Lipo, DMPC/DO-Lipo, and LM-Lipo prepared by incubation with HL-60 cells (ATRA (-) or ATRA (+)) were added onto untreated (A and D) or TNF-α-treated HUVECs (B and E), and the cells were incubated for 3 h at 37ºC. Thereafter, the cells were fixed, and their nuclei were

counterstained with DAPI. Fluorescence images were obtained by fluorescence microscopy. DiI (liposome; red, upper column) and merged images (lower column) of DAPI (nuclei; blue), DiI, and phase contrast are shown. Scale bars = 100 μm. (C, F) HUVECs (5 x 10^4 cells/well onto 24-well plate) were incubated with EGM-2 containing TNF-α (10 ng/mL) for 16 h at 37ºC. TNF-α-treated and untreated HUVECs were then treated with the indicated DiI-labeled liposomes for 3 h at 37ºC. After lysis of the cells, the fluorescence intensity of DiI in the cells was measured. The relative fluorescence intensity of each group to that in control (C: EPC/DO-Lipo, F: DMPC/DO-Lipo) are presented. The data show the mean ± S.D. (n=4). Statistical differences were calculated by ANOVA with Tukey *post-hoc* test. Significant differences; * $P<0.05$, $^{\#}P<0.05$, $^{\#\#}P<0.01$ vs. DMPC/DO-Lipo, $^{\#\#\#}P<0.001$ vs. EPC/DO-Lipo. These experiments were performed 4 times independently.

Figure 5. Passage of leukocyte-mimetic liposomes through inflamed endothelial cell layer.

HUVECs seeded on a Transwell plate (2 x 10^5 cells/inserts) were cultured for 48 h at 37ºC, followed by incubation with TNF-α (10 ng/mL) for 16 h at 37ºC. Next, DiI-labeled EPC/DO-Lipo or LM-EPC/DO-Lipo (ATRA (-) or (+)) was added (50 nmol as lipid dose/insert, 100 μL of each liposome at a concentration of 0.5 mM diluted with EBM-2) onto the upper compartment of the Transwell plate and incubated for 3 h at 37ºC. Thereafter, the fluorescence intensity of DiI in the media of the bottom compartment was measured. The relative fluorescence intensity of each group to that in control (EPC/DO-Lipo) are presented. The data show the mean ± S.D. (n = 20). Statistical differences were calculated by ANOVA with Tukey *post-hoc* test. Significant difference; * $P<0.05$ vs. EPC/DO-Lipo. The experiment was performed 5 times independently, and the sum of the data of each experiment is shown.

Figure 6. Effect of treatment with leukocyte-mimetic liposomes on the actin cytoskeleton in TNF-α-treated HUVECs.

(A-D) HUVECs (1 x 10^5 cells) grown on 35-mm glass-bottom dishes were treated with

TNF-α (10 ng/mL in EGM-2 medium) for 16 h at 37ºC. The cells were then treated with DiI-labeled EPC/DO-Lipo or leukocyte-mimetic liposomes (LM-EPC/DO-Lipo (ATRA (-) or ATRA (+)) for 3 h at 37ºC. The cells were then fixed with 4% PFA, permeabilized with PBS containing 0.1% TritonX-100, and incubated with 1% BSA in PBS, followed by staining with Alexa Fluor 488-conjugated phalloidin solution. Finally, the nuclei of the cells were stained with DAPI, and the fluorescence was observed using a confocal laser scanning microscope. Images were obtained from untreated (TNF-α (-)) HUVECs (A), or TNF-α-treated HUVECs treated with plain liposomes (B), LM-EPC/DO-Lipo (ATRA (-)) (C), or LM-EPC/DO-Lipo (ATRA (+)) (D). Blue, green, and red colors represent the individual fluorescence of DAPI (nuclei), Alexa Fluor 488 (F-actin) and DiI (liposome), respectively. Scale bars = 20 μm. The experiment was independently performed 4 times, all of which showed similar profiles.

Figure 7. Influence of leukocyte-mimetic liposomes on the intercellular adhesion protein VE-cadherin in inflamed endothelial cells.

(A-D) TNF-α-treated HUVECs were treated with each liposome according to the same procedure described in the legend of Fig. 6. After removing the liposomal samples, the cells were fixed with 4% PFA and permeabilized with PBS containing 1% BSA and 0.1% Triton X-100. Thereafter, the cells were incubated with anti-VE cadherin antibody for 1 h at 37ºC, followed by incubation with Alexa Fluor 488-conjugated secondary antibody for 1 h at 37ºC. After staining the nuclei with DAPI, fluorescence images were obtained from untreated HUVECs (A), and TNF-α-treated HUVECs treated with the indicated liposomes (B-D) by confocal laser scanning microscopy. Blue and green colors show the fluorescence of DAPI (nuclei) and Alexa Fluor 488 (VE-cadherin), respectively. Scale bar = 20 μm. The experiments were performed 5 times independently. (E) The relative fluorescence intensity of VE-cadherin positive area between cell borders to that in control was calculated from over 8 or more images per each group of HUVECs for one experiment by using ImageJ. The data show the mean ± S.D. (n=5). Statistical differences were

analyzed by ANOVA with Tukey *post-hoc* test. Significant differences; ### $P<0.001$ vs. Control (TNF-α (-)), * $P<0.05$ vs. EPC/DO-Lipo (TNF-α (+)).

Fig. 1

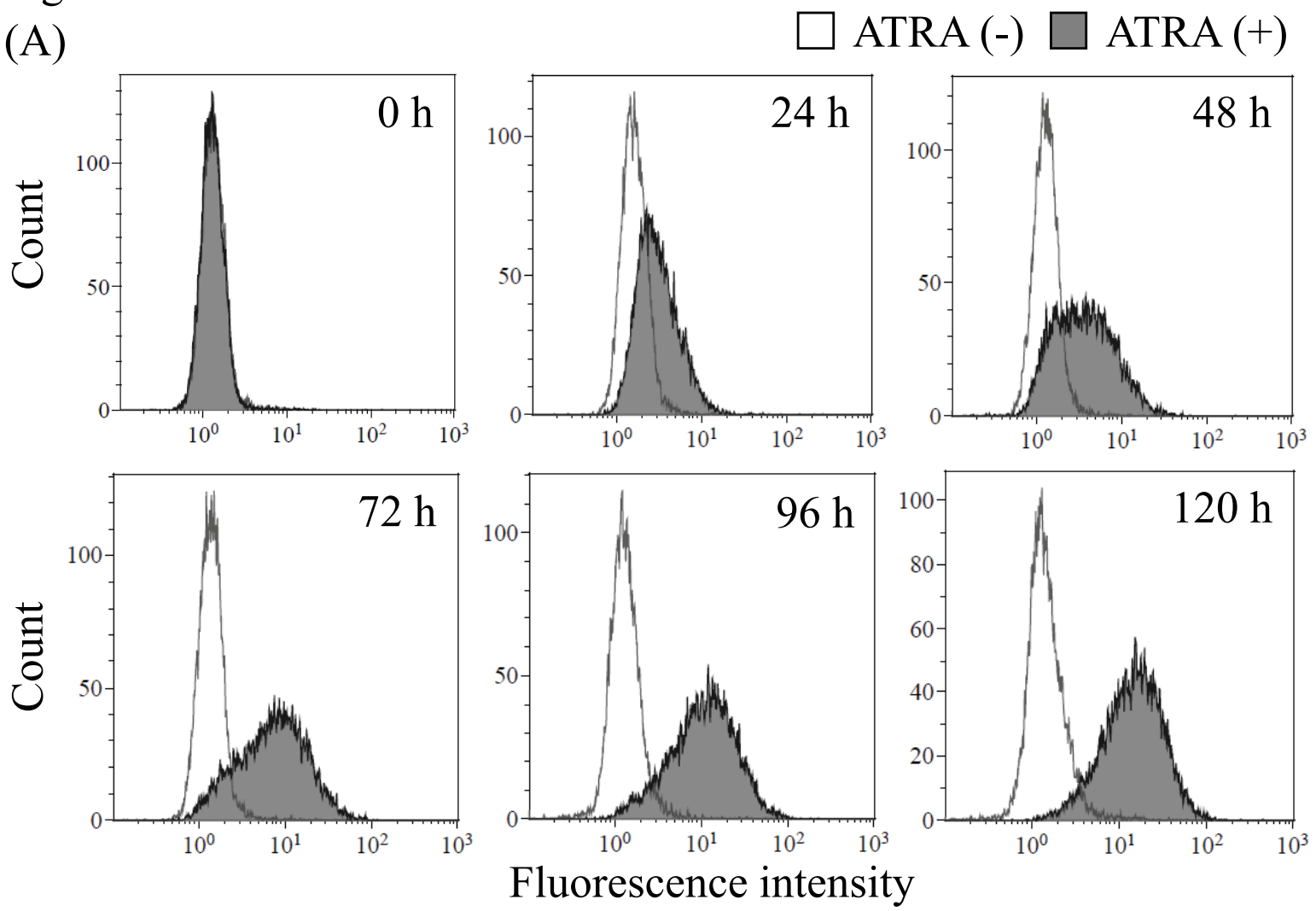
(A)
ATRA (-)
ATRA (+)
0 h
24 h
48 h
72 h
96 h
120 h
Count
Count
Fluorescence intensity

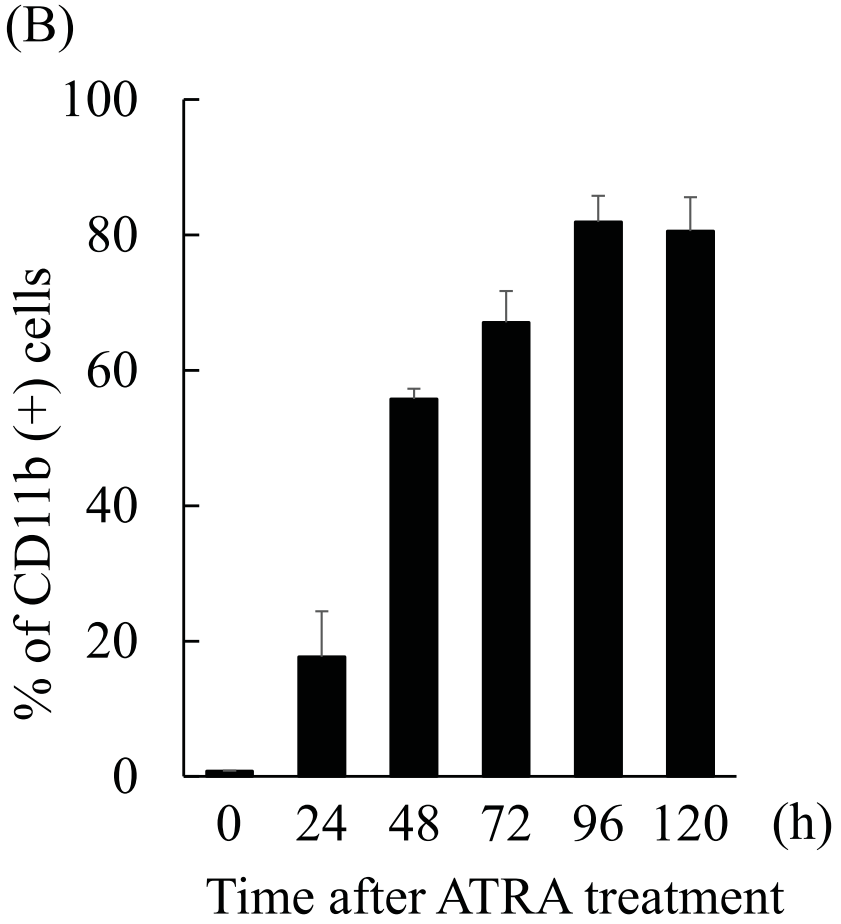
(B)
% of CD11b (+) cells
Time after ATRA treatment
0
24
48
72
96
120
(h)

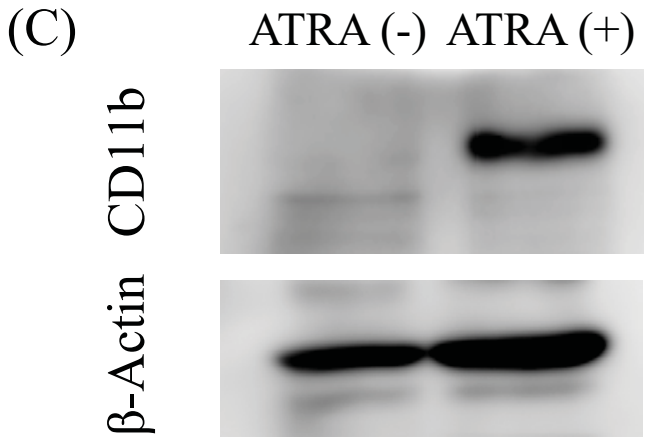
(C)
ATRA (-)
ATRA (+)
CD11b
β-Actin

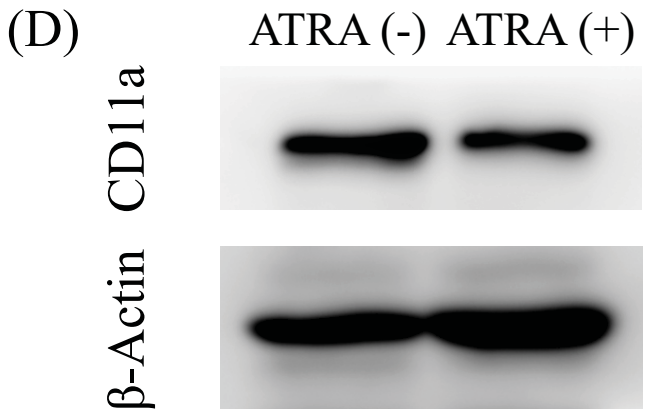
(D)
ATRA (-)
ATRA (+)
CD11a
β-Actin

Fig. 2

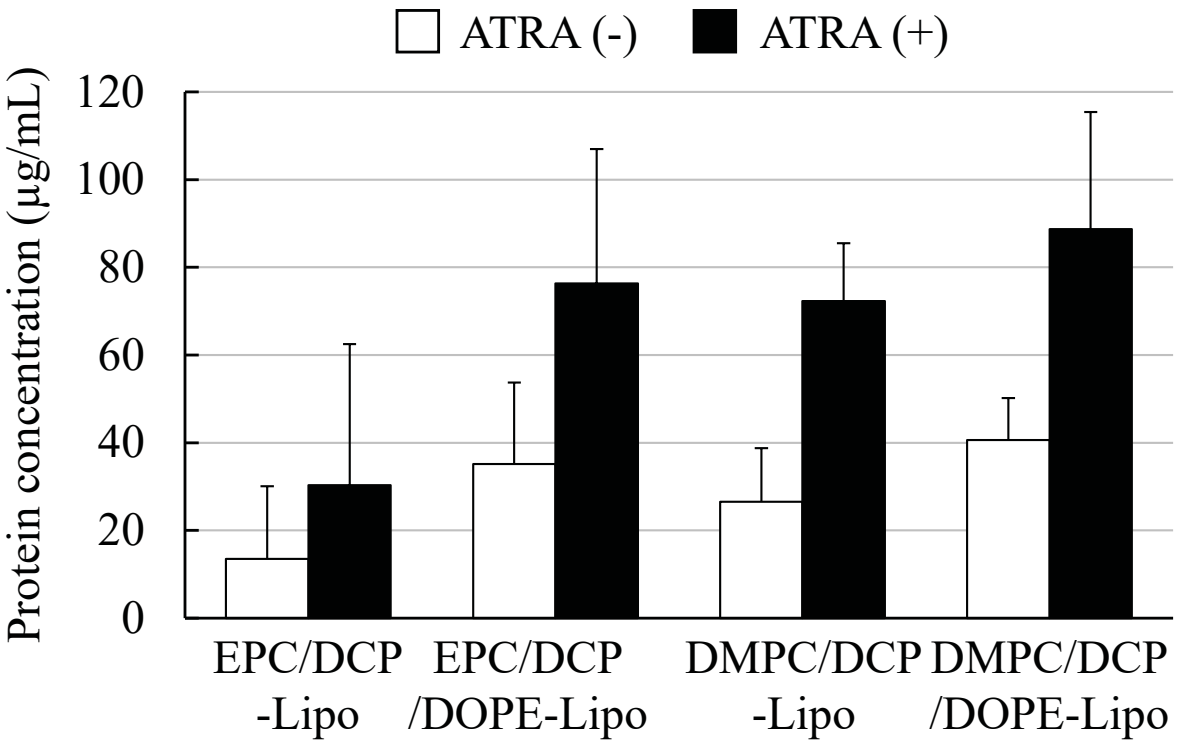
ATRA (-)
ATRA (+)
Protein concentration (μg/mL)
120
100
80
60
40
20
0
EPC/DCP -Lipo
EPC/DCP /DOPE-Lipo
DMPC/DCP -Lipo
DMPC/DCP /DOPE-Lipo

Fig. 3

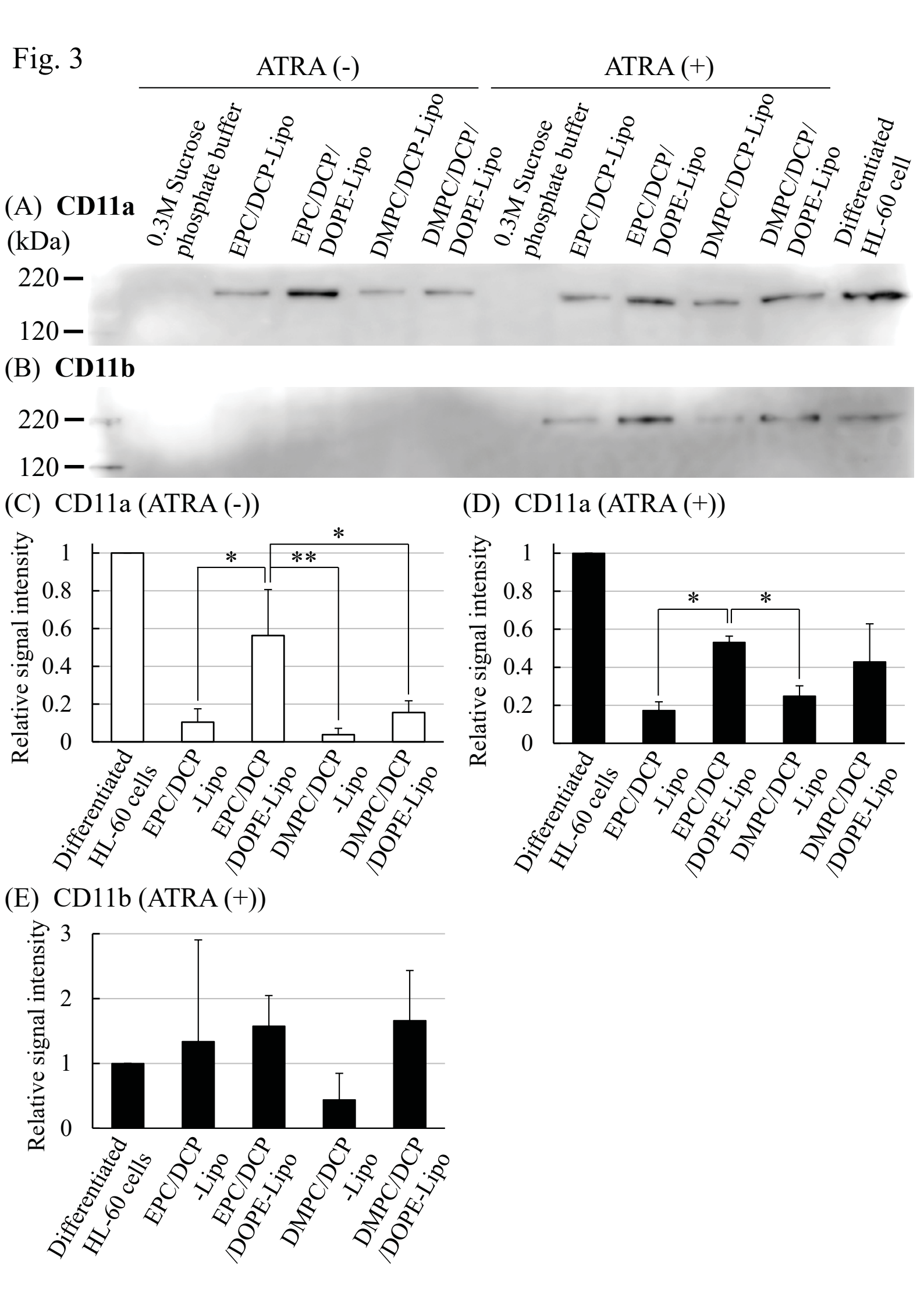
ATRA (-)
ATRA (+)
0.3M Sucrose phosphate buffer
EPC/DCP-Lipo
EPC/DCP/ DOPE-Lipo
DMPC/DCP-Lipo
DMPC/DCP/ DOPE-Lipo
Differentiated HL-60 cell
(A) CD11a
(kDa)
220
120
(B) CD11b
220
120
(C) CD11a (ATRA (-))
Relative signal intensity
0
0.2
0.4
0.6
0.8
1
*
**
*
Differentiated HL-60 cells
EPC/DCP -Lipo
EPC/DCP /DOPE-Lipo
DMPC/DCP -Lipo
DMPC/DCP /DOPE-Lipo
(D) CD11a (ATRA (+))
Relative signal intensity
0
0.2
0.4
0.6
0.8
1
*
*
Differentiated HL-60 cells
EPC/DCP -Lipo
EPC/DCP /DOPE-Lipo
DMPC/DCP -Lipo
DMPC/DCP /DOPE-Lipo
(E) CD11b (ATRA (+))
Relative signal intensity
0
1
2
3
Differentiated HL-60 cells
EPC/DCP -Lipo
EPC/DCP /DOPE-Lipo
DMPC/DCP -Lipo
DMPC/DCP /DOPE-Lipo

Fig. 4

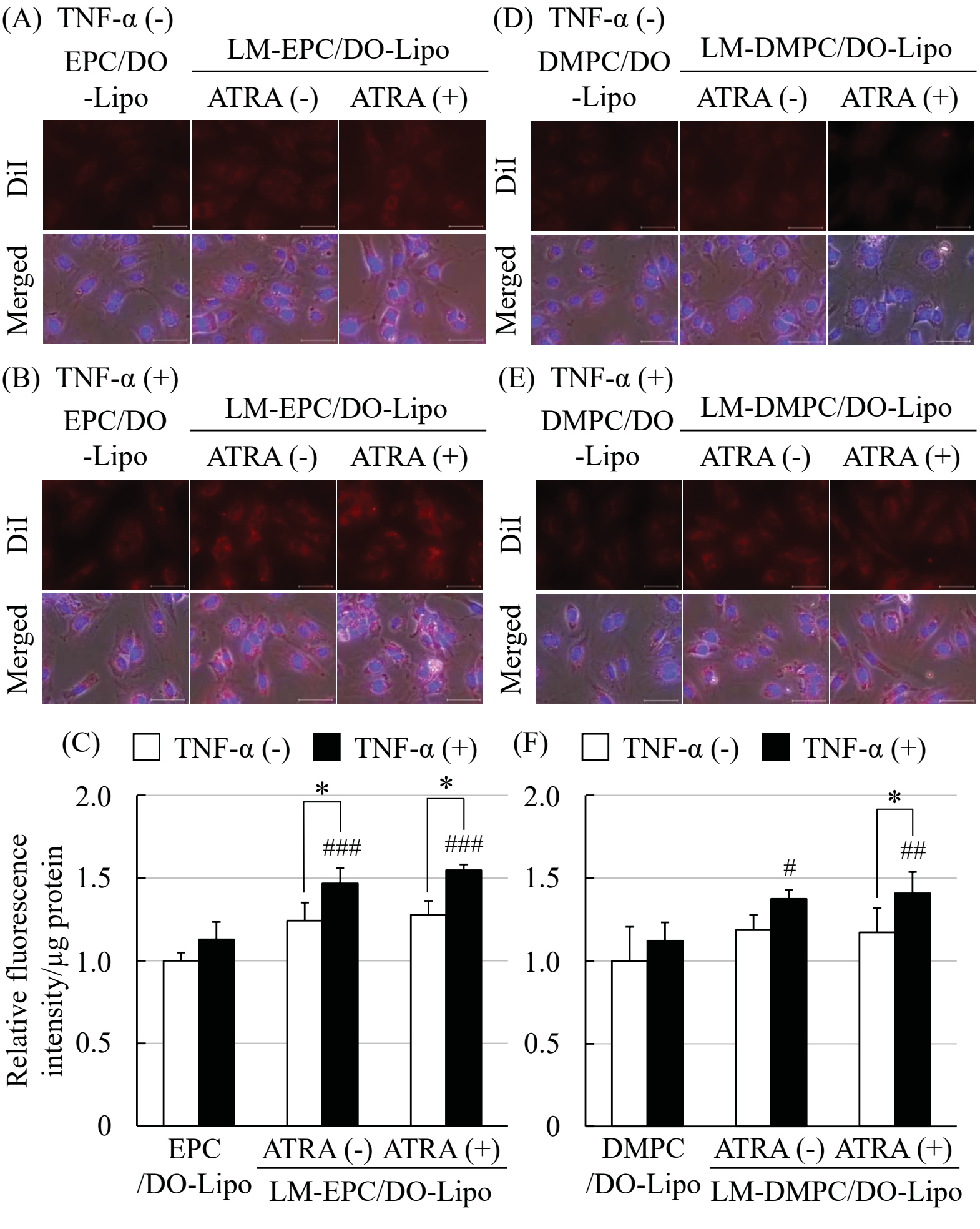
(A) TNF-α (-)
EPC/DO -Lipo
LM-EPC/DO-Lipo
ATRA (-)
ATRA (+)
DiI
Merged
(D) TNF-α (-)
DMPC/DO -Lipo
LM-DMPC/DO-Lipo
ATRA (-)
ATRA (+)
DiI
Merged
(B) TNF-α (+)
EPC/DO -Lipo
LM-EPC/DO-Lipo
ATRA (-)
ATRA (+)
DiI
Merged
(E) TNF-α (+)
DMPC/DO -Lipo
LM-DMPC/DO-Lipo
ATRA (-)
ATRA (+)
DiI
Merged
(C)
TNF-α (-)
TNF-α (+)
Relative fluorescence intensity/μg protein
2.0
1.5
1.0
0.5
0
*
*
###
###
EPC /DO-Lipo
ATRA (-)
ATRA (+)
LM-EPC/DO-Lipo
(F)
TNF-α (-)
TNF-α (+)
2.0
1.5
1.0
0.5
0
*
#
##
DMPC /DO-Lipo
ATRA (-)
ATRA (+)
LM-DMPC/DO-Lipo

Fig. 5

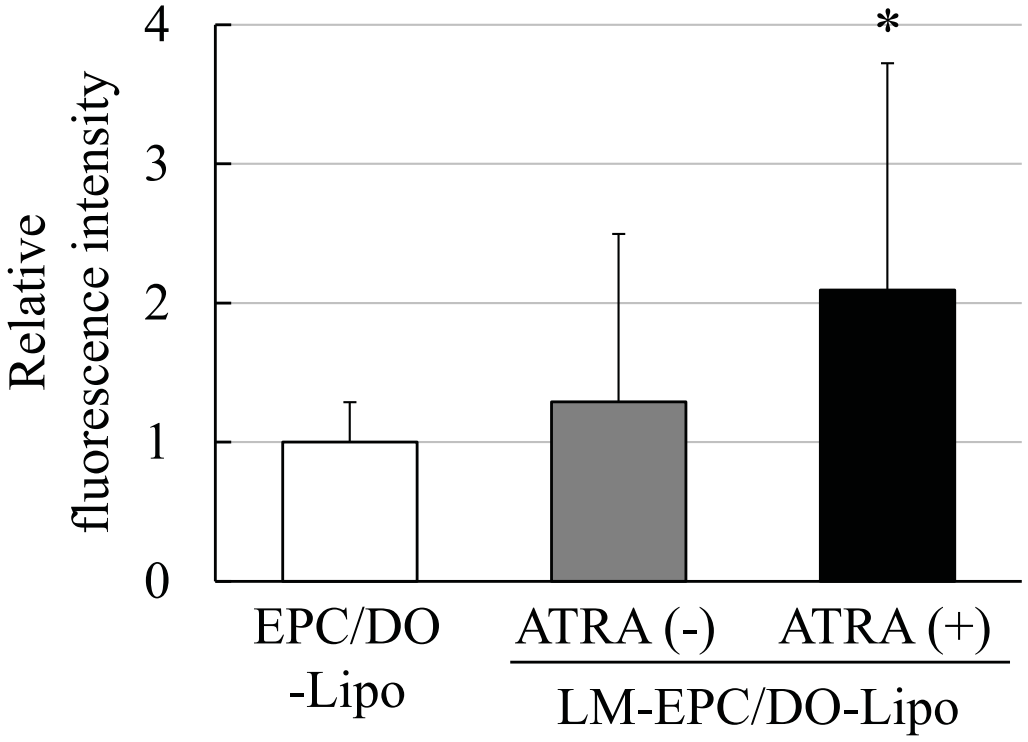
Relative fluorescence intensity
4
3
2
1
0
*
EPC/DO -Lipo
ATRA (-)
ATRA (+)
LM-EPC/DO-Lipo

Fig. 6

(A) Control (TNF-α (-))

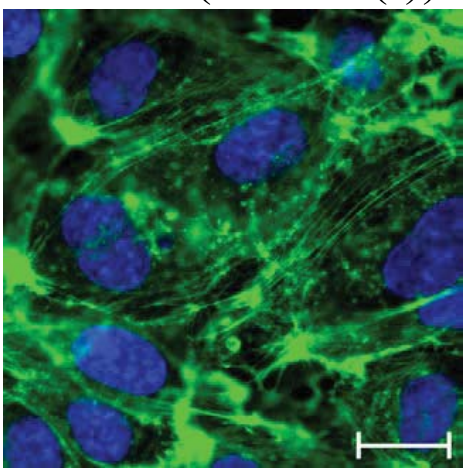

(B) EPC/DO-Lipo

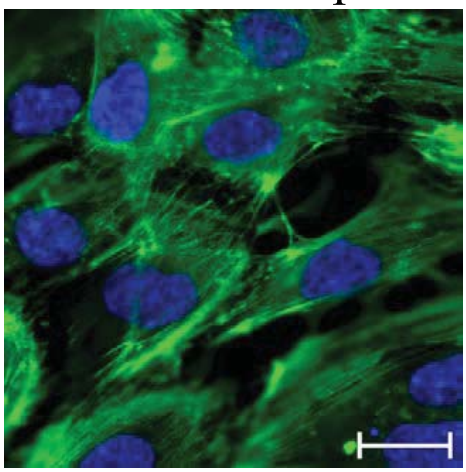

(C) LM-EPC/DO-Lipo
ATRA (-)

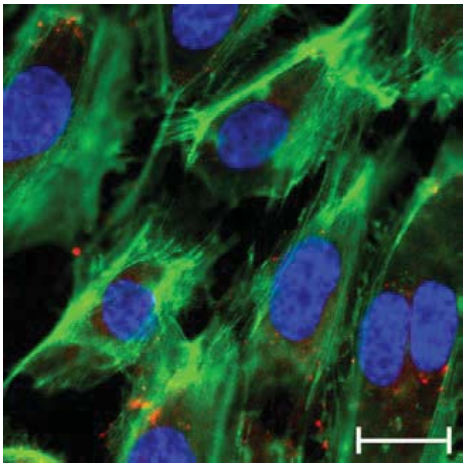

(D) LM-EPC/DO-Lipo
ATRA (+)

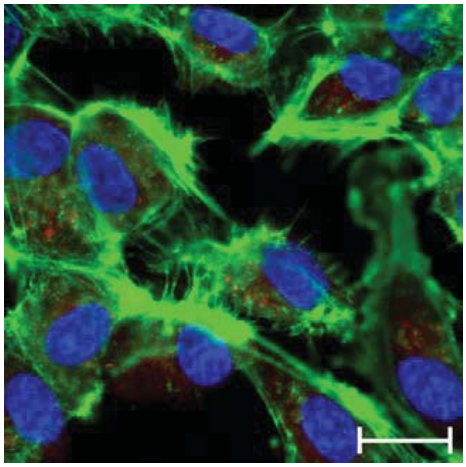

Fig. 7

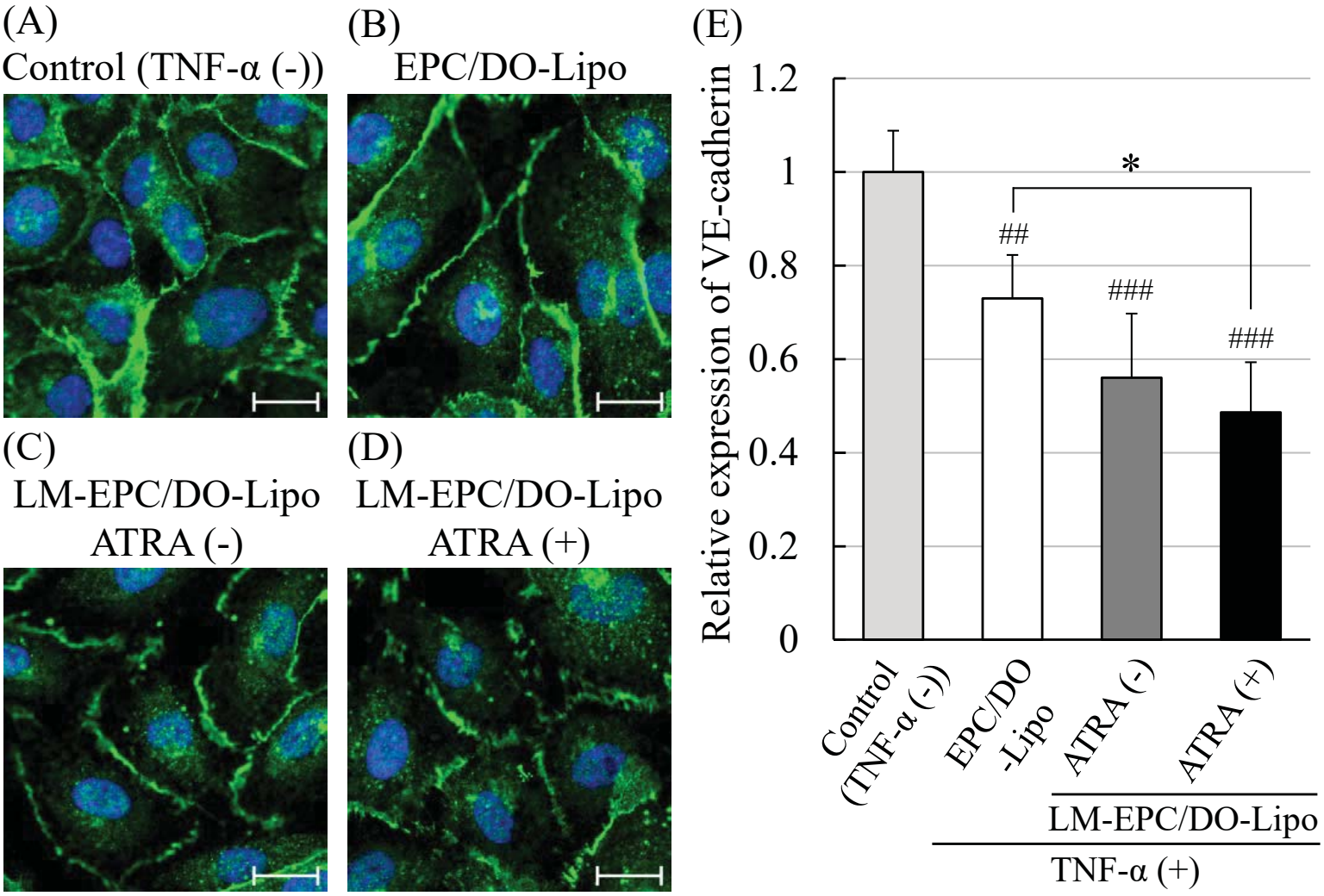
(A)
Control (TNF-α (-))
(B)
EPC/DO-Lipo
(C)
LM-EPC/DO-Lipo
ATRA (-)
(D)
LM-EPC/DO-Lipo
ATRA (+)
(E)
Relative expression of VE-cadherin
1.2
1
0.8
0.6
0.4
0.2
0
*
##
###
###
Control (TNF-α (-))
EPC/DO -Lipo
ATRA (-)
ATRA (+)
LM-EPC/DO-Lipo
TNF-α (+)